A High Dynamic Range Amplifier for Wideband Active Loop Antennas

by

Chris Trask / N7ZWY
Sonoran Radio Research
P.O. Box 25240
Tempe, AZ 85285-5240

Senior Member IEEE

Email: christrask@earthlink.net

2 August 2010
Revised 3 August 2010
Revised17 August 2010

Introduction

Loop antennas are of interest to a wide range of users, from shortwave listeners (SWLs) and radio amateurs to designers of direction-finding receiver systems. SWLs and radio amateurs living in confined areas such as apartments or in communities having antenna restrictions find loop antennas and especially active loop antennas to be a practical solution as they can offer directional performance similar to that of a dipole antenna while taking up a considerably smaller space, and their small size makes them readily adaptable to mechanical rotation. In addition, shielded loop antennas also provide a good degree of immunity from low-frequency magnetic field interference

Remote tuning is often employed to overcome the high inductive reactance of the loop antenna impedance for achieving good performance and enjoying the highly desireable magnetic field response, which provides some degree of immunity from electric field noise from sources such as lightning discharges, faulty mains transformers, and flourescent lighting. Many users, however, find remote tuning to be inconvenient and instead prefer to use loop antennas with a wide bandwidth. This requires an amplifier that has a very low input impedance so that the loop antenna is seen as a current source.

Loop Antenna Impedance

Before we address the design of wideband loop antenna amplifiers, we need to gain an understanding and appreciation of the impedance of loop antennas, the nature of which is typically a serious obstacle for users of loop antennas. It is well known that the loop antenna impedance consists of a small real part R_{ant} (consisting of the radiation resistance plus bulk and induced losses) in series with a large inductance L_{ant}, which renders the loop antenna as being a high Q source (1):

$$Q_{ant} = \frac{\omega L_{ant}}{R_{ant}} \quad (1)$$

where ω is the frequency in radians per second.

There is more than enough literature available about loop antennas that the basic theory really does not need to be repeated here, and very thorough treatments are available from King (2), Kraus (3), Terman (4) and Padhi (5). Most authors provide little discussion about the impedance of the loop antenna, other than to demonstrate that the impedance is dominated by a large series inductance and is a cascade of parallel and series resonances (6). A few go further and show that the loop antenna impedance can be seen as a shorted transmission line. Terman (4) makes use of such a method, which is usable for frequencies below the first parallel resonance.

An IEEE paper published in 1984 (7), provides a very useful means for estimating the real and imaginary parts of the loop antenna impedance, the latter of which is a refinement of the method proposed by Terman, and which the authors of that paper further refine by providing scalar coefficients for use with a wide variety of geometries that are commonly used in the construction of loop antennas. In their approximation, the radiation resistance is determined by:

$$R_{ant} = a\, tan^{b}\left(\frac{k_0 L}{2}\right) \quad (2)$$

where L is the perimeter length of the loop antenna and the wave number k_0 is defined as:

$$k_0 = \omega\sqrt{\mu_0 \varepsilon_0} \quad (3)$$

where μ is the permeability of free space ($4 \pi 10^{-7}$ H/m), and ε is the permittivity of free space ($8.8542\ 10^{-12}$ F/m). The coefficients *a* and *b* in Eq. 2 are dependent on the geometry and the

Configuration	$L/\lambda \leq 0.2$		$0.2 \leq L/\lambda \leq 0.5$	
	a	b	a	b
Circular	1.793	3.928	1.722	3.676
Square (side driven)	1.126	3.950	1.073	3.271
Square (corner driven)	1.140	3.958	1.065	3.452
Triangular (side driven)	0.694	3.998	0.755	2.632
Triangular (corner driven)	0.688	3.995	0.667	3.280
Hexagonal	1.588	4.293	1.385	3.525

Table 1 - Coefficients to be Used with Equation 2

perimeter length of the loop antenna, a list of values being provided in Table 1.

The inductive reactance of the loop antenna impedance is determined by:

$$X_{ant} = j\, Z_0\, tan\left(\frac{k_0\, L}{2}\right) \qquad (4)$$

where Z_0 is the characteristic impedance of the equivalent parallel wire transmission line, defined as:

$$Z_0 = 276\, ln\left(\frac{4\, A}{L\, r}\right) \qquad (5)$$

where A is the enclosed area of the loop antenna and r is the radius of the antenna conductor.

A highly detailed report from the Ohio State University Electroscience Laboratory in 1968 (8) provides a thorough analytical means for estimating the real and imaginary parts of the impedance of single and multi-turn loop antennas, as well as the antenna efficiency.

Computer simulation routines such as EZNEC also provide a useful means for estimation the loop antenna impedance. Together with papers and reports such as those mentioned herein, they allow the designer to gain an understanding of the nature of the loop antenna impedance. They are not, however, suitable substitutes for actual measurements and the designer should always rely to measured data, especialy when designing matching networks.

Fig. 1 shows the measured terminal impedance of a 1m diameter loop made with 0.25" copper tubing. In order to ensure that the loop antenna is properly balanced, a 1:1 BalUn transformer is used to interface the loop antenna with the impedance bridge. Loop antennas that are fed unbalanced have dramatically different impedance characteristics and radiation patterns from those that are fed balanced (9).

For the purpose of discussion it is very useful to devise lumped element equivalent models as some analysis and optimization routines, such as PSpice, do not have provisions for including tables of measured data for interpolation. Fig. 2 illustrates two simplified lumped

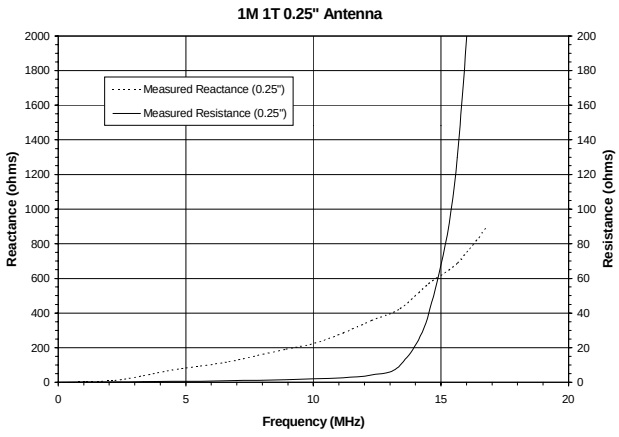

Fig. 1 - Measured Impedance of 1 meter Diameter Loop Antenna made with 0.25" Copper Tubing

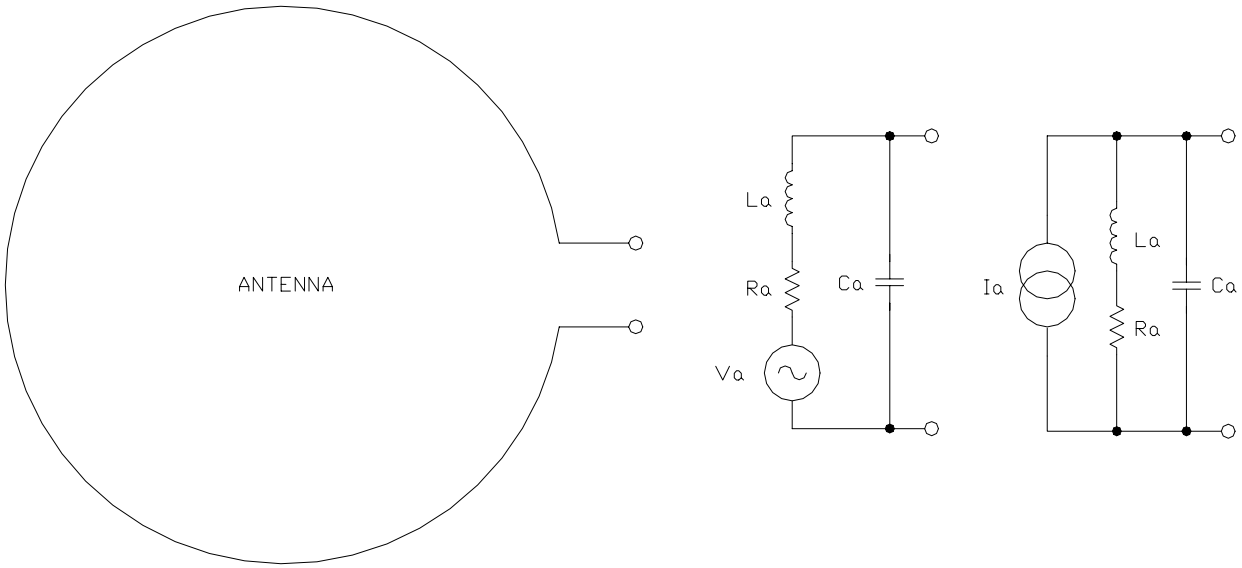

Fig. 2 - The Loop Antenna (left) Together with Simplified Lumped Element Thevenin (centre) and Norton (right) Impedance Models.

element models, the first being a Thevenin equivalent with a voltage signal source, and the second being a Norton equivalent with a current signal source. Far more detailed models can be devised that include subsequent resonances and anti-resonances (10), but they would serve little purpose here.

The Norton equivalent model of Fig. 2 shows the loop antenna impedance in a form that shows that a load with a very low resistance would be an ideal termination for the loop antenna. Amplifiers having this characteristic are somewhat difficult to design.

What's All This Passive Augmentation Stuff, Anyhow?

Augmentation is a patented circuit topology that reduces the emitter input impedance of a common-base bipolar transistor amplifier by detecting the signal voltage at the emitter, then amplifiying and inverting it and applying it to the base. Augmentation can be implemented passively with a 2-winding (simple) or 3-winding (compound) transformer, actively with a common-emitter amplifier, as well as a combining of the two methods known as tandem augmentation. The method has been shown in numerous publications to improve the linearity and noise figure (NF) characteristics of common-base small-signal and power amplifiers (11, 12, 13, 14, 15).

The basic concept of simple passive augmentation is shown in Fig. 3. Here a 2-winding transformer T1 detects the input signal voltage across the primary winding, amplifies the magnitude by the turns ratio N, inverts the result, and applies it to the transistor base. For a simple

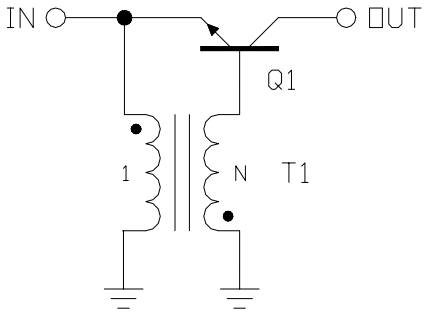

Fig. 3 - Basic Concept of Simple Passive Augmentation

common-base amplifier without augmentation, the incremental emitter input resistance r_e is determined by:

$$r_e = \frac{v_E}{i_E} \approx \frac{v_E}{I_0 \, \varepsilon^{\frac{q\,v_E}{kT}}} \tag{6}$$

where v_E is the incremental input voltage, I_O is the transistor reverse saturation current, q is the electronic charge (1.60219×10^{-19} J), k is Boltzmann's constant (1.380622×10^{-23} J/K), and T is the temperature in degrees Kelvin (K). In Fig. 3, the input voltage v_E and the transistor base-emitter voltage v_{BE} are related by:

$$v_{BE} = v_B - v_E = N\,v_E - v_E = \\ = -v_E(N+1) \tag{7}$$

Knowing that the transistor base and emitter incremental currents i_B and i_E are related by:

$$i_B = \frac{i_E}{h_{fe}} \tag{8}$$

where h_{fe} is the current gain of the transistor, we can dertermine that the signal input current i'_E of Fig. 3 is:

$$i'_E = i_E - N\,i_B = i_E - N\frac{i_E}{h_{fe}} = \\ = i_E\left(1 - \frac{N}{h_{fe}}\right) \tag{9}$$

Substituting Eq. 7 and Eq. 9 into Eq. 6, we can now determine that the incremental input resistance r'_e of the passively augmented common-base amplifier of Fig. 3 is:

$$r'_e = \frac{v_E}{i'_E} \approx \\ \approx \frac{v_E}{\left(1 - \frac{N}{h_{fe}}\right) \times I_0 \, \varepsilon^{\frac{q\,v_E(N+1)}{kT}}} \tag{10}$$

As shown in Fig. 4, a transformer ratio of just 2:1 can result in an 85% reduction in the amplifier input resistance, while a transformer ratio of 3:1 results in a 94% reduction. Together with the improved IMD and NF performance, the substantial decrease in the amplifier input resistance is of great benefit to the design of wideband active loop antenna amplifiers.

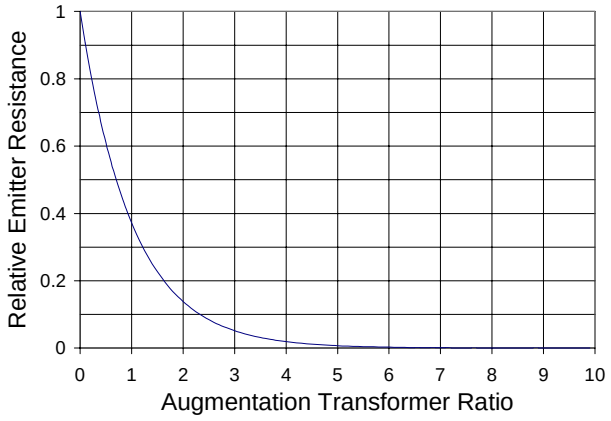

Fig. 4 - Relative Emitter Input Impedance with Passive Augmentation (h_{fe} = 100)

In compound passive augmentation, shown in Fig. 5, a third winding of ratio M is added to the transformer. The primary winding now becomes an autotransformer having a current gain of 1+M, and usinga development similar to that for simple passive augmentation the input impedance is determined as:

$$r'_e \approx \frac{v_E\,(1+M)^2}{\left(1 - \frac{N}{h_{fe}}\right) \times I_0 \, \varepsilon^{\frac{q\,v_E(N+1)}{kT}}} \tag{11}$$

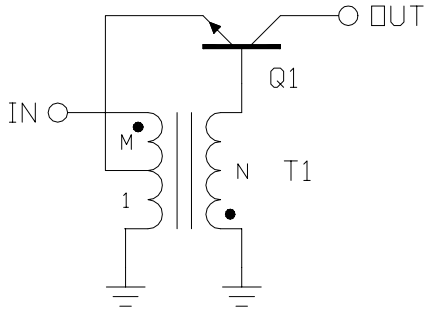

Fig. 5 - Basic Concept of Compound Passive Augmentation

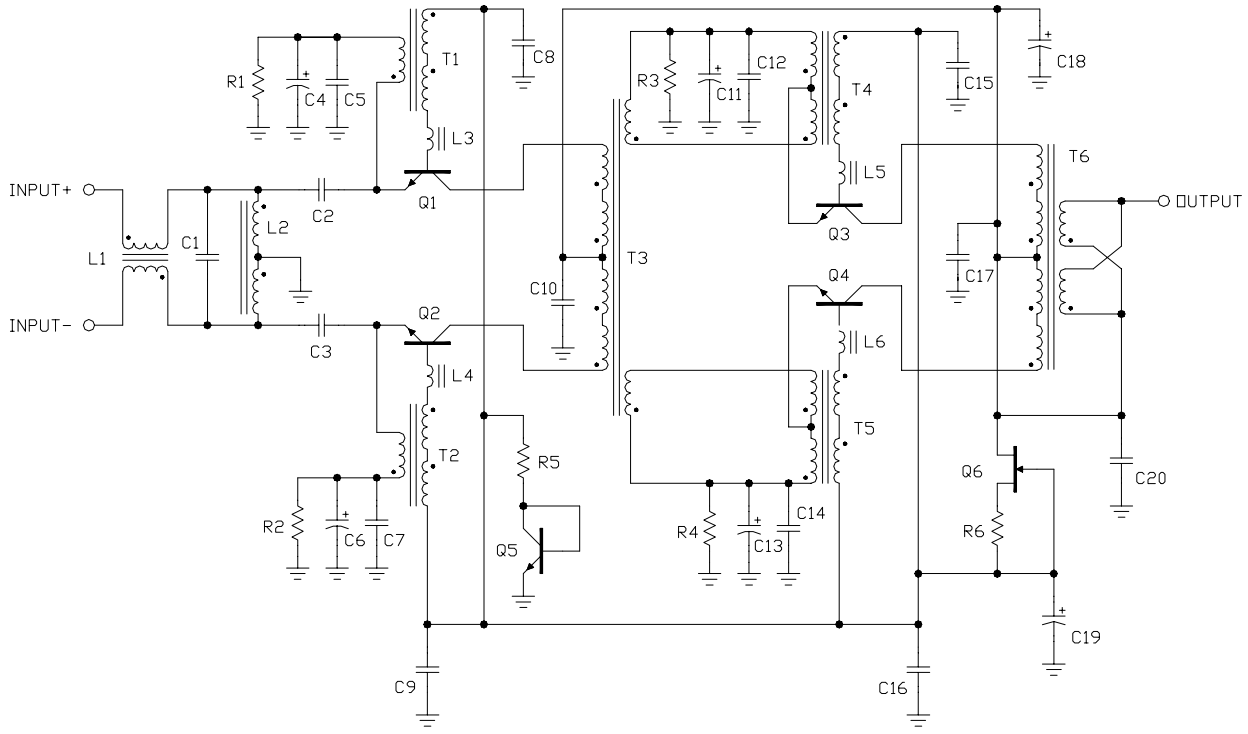

C1 - 2700pF Mica (optional, see text)
C2, C3 - 0.10uF low ESR (Kemet C1206C104K3HACTU or equivalent)
C4, C6, C11, C13, C19 - 22uF 6.3WVDC tantalum (Kemet T520A226M006ATE100 or equivalent)
C5, C7, C12, C14 - 0.1uF 25V low ESR (Kemet C1206C104K3HACTU or equivalent)
C8, C9, C10, C15, C16, C17, C20 - 0.1uF 25V
C15 - 47uF 50WVDC aluminum

L1 - 4.7nH (optional, see text)
L2 - 82nH (see text)
L3, L4, L5, L6 - Ferrite Bead (see text)

Q1, Q2, Q3, Q4, Q5 - MPS6521
Q6 - PN4416

R1, R2 - 47 ohms
R3, R4 - 33 ohms
R5 - 150 ohms
R6 - 68 ohms

T1, T2 - 1:2 on 2843002402 balun core (see text)
T3, T6 - 2:2:1:1 on 2861000102 balun core (see text)
T4, T5 - 1:1:2 on 2843002402 balun core (see text)

Fig. 6 - Wideband Loop Antenna Amplifier Schematic and Parts List

Note in Eq. 11 that the consequence of compound passive augmentation is that the input resistance will be increased by the square of 1+M.

In practice, it has been found that in compound passive augmentation the performance is often best when the turns ratio N is equal to 1+M, which is very convenient in the construction of the transformer, which will be discussed later.

Amplifier Design

The schematic for the wideband active loop antenna amplifier is shown in Fig. 6. In the concept of the the design, due consideration needed to be given to a number of factors regarding performance and cost.

First of these is the suppression of common-mode signals that can result from a multitude of external sources, such as lightning discharges. Inductors L1 and L2 provide the first line of defense from this form of interference, and needs to be constructed in such a manner that the balance is maintained without having to resort to practices that are beyond those of average ability.

Additional souces of common-mode interference include even-order distortion due to non-linear transfer characteristics in both the transistors and the transformers, the latter due to premature flux saturation in the core material. The use of balanced stages helps to suppress even-order distortion, and this requires that transformers T3 and T6 also be constructed to ensure good balance.

The degradation of NF due to transistor noise and resistive losses needs to be minimized. In low-impedance circuitry this latter source of noise degredation becomes a bit problematic, and in this case requires that capacitors C2 and C3 be chosen to have exceptionally low equivalent series resistance (ESR). In addition, inductor L1 and transformer T4 need to be constructed so as to minimize bulk and induced losses.

The first stage uses simple passive augmentation, consisting of transformers T1 and T2 so as to provide the lowest input impedance possible as well as minimize both NF and IMD. The second stage uses compound passive augmentation, consisting of transformers T4 and T5 so as to provide additional current gain as well as minimize IMD.

Low-frequency performance is limited by the coupling coefficient of transformer T3 due to the low impedance of that stage, and adds further to the attention that needs to be brought to bear on its design and construction. Otherwise, low frequency cutoff is determined primarily by by L2, C2, and C3 in the input roofing filter.

L2 is constructed in such a way as to ensure that the amplifier input is balanced so that the desireable radiation pattern null of the loop antenna is not impaired. As mentioned earlier, it also seves to suppress common-mode signals.

High-frequency perfomance is limited by the collector-base and output capacitances (C_{CB} and C_O, respectively) of transistors Q3 and Q4, each of which see a load resistance of 400 ohms, thereby forming the majority pole of the amplifier. The load resistances seen by transistors Q1 and Q2 are kept low so as to not provide additional poles that would impair the high frequency performance. To a lesser degree, the leakage inductances of transformers T3 and T6 also add to the impairment of the high-frequency performance.

In the roofing filter, L1 and C1 determine the high cutoff frequency of the amplifier. Just as with L2, L1 is constructed in such a way as

to ensure that the amplifier input is balanced, as well as to supress common-mode signals. If interference from local TV and FM broadcasters is not a problem, L1 and C1 need not be used.

It was decided at the beginning of the design that the secondary winding(s) of transformer T6 be used to conduct the DC power from the feedline to the amplifier circuitry, rather than add a large choke and isolating the secondary by way of blocking capacitors. In order that flux saturation be avoided due to the bias flux that would result from this approach, a core with a sufficiently large cross section would be required. This is not an issue for T3 as the bias flux resulting from DC passing through its windings cancel, as do the bias fluxes resulting from DC passing through the primary windings of T6, providing that the bias currents are reasonably equal.

Low-frequency performance is also dependent on the quality of the bypass capacitors in the emitter circuits. As with the constraints placed in the design of transformer T3, these capacitors need to have low ESR. This requirement is probably obvious with respect to the 0.1uF capacitors, but not necessarily for the 22uF electrolytics. Most designers are familiar with the high-frequency products of even-order intermodulation (1x1, 2x2, etc.) but rarely take the low-frequency products into consideration. These low-frequency products, if not properly bypassed, can modulate the biasing of an amplifier and in turn lead to further degredation of the in-band IMD performance. The capacitors suggested in the parts list were chosen as they provide good ESR performance at a reasonable cost and are readily available from popular retail distributors

Ferrite beads L3, L4, L5, and L6 are included to suppress VHF oscillations and are placed on the base leads of the transistors. Although there is no need to be precise about their selection, small beads made from a good quality high frequency material similar to Fair-Rite 43 or 61 should be considered first so as to have little effect at HF frequencies.

Transistor Q6 provides a temperature-stable constant-current source which is adjusted by resistor R6. Transistor Q5 serves as a reference diode and with resistor R5 provides a temperature-sensitive base voltage for the amplifier transistors. These four devices serve to keep the amplifier bias stable over temperature.

Transistor Selection

The MPS6521 transistors used in the design have very high gain, and when combined with passive augmentation the distortion is decreased and the balance is improved. They also have good NF performance, and as shown in Fig. 7 they have very good transistion and saturation characteristics, which translates into good linearity and compression (P_{1dB}).

The PN4416 JFET was chosen for Q6 as

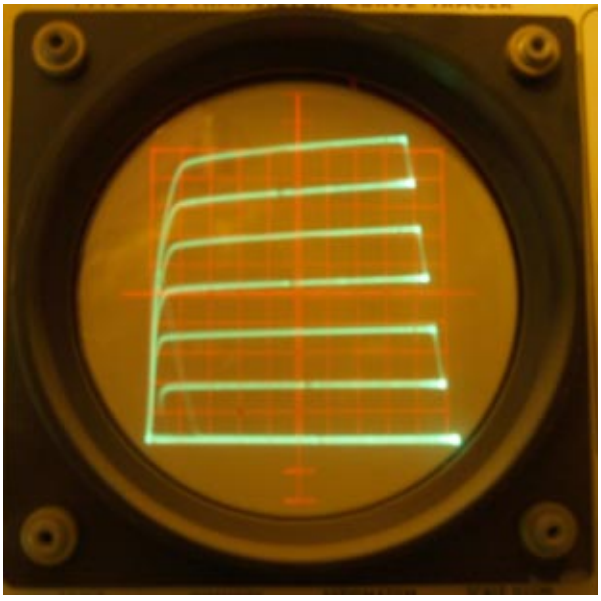

Fig. 7 - MPS6521 Voltage and Current Characteristics (20 μA/step, vertical - 5mA/div, horizontal - 1V/div)

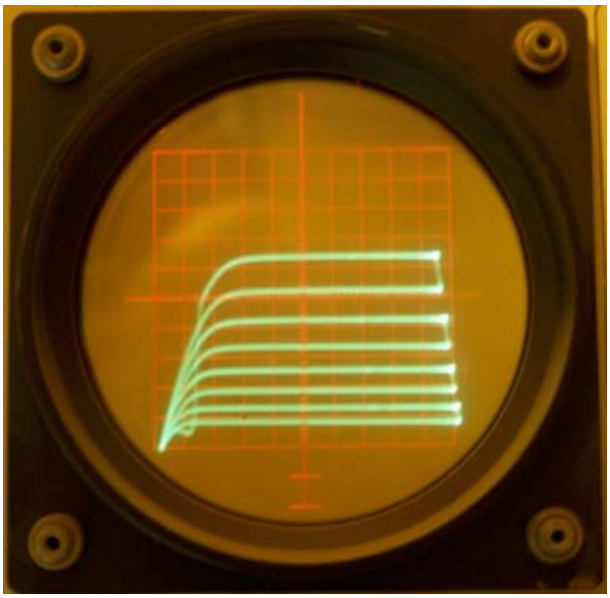

Fig. 8 - PN4416 Voltage and Current Characteristics (200mV/step, vertical - 1mA/div, horizontal - 1V/div)

the drain current (I_D) remains very stable over a wide range of drain-source voltage (V_{DS}), as shown in Fig. 8. This provides a great deal of immunity from power supply noise. It is also a very quiet device, and these combined characteristics provide a much quieter base voltage source than can be obtained from popular three-teminal regulators such as the LM78L05.

Transformer Construction

The Mini-Circuits T4-6T may be used for the first stage augmentation transformers T1 and T2, however a much better performing transformer is easily made with four turns of #32 trifilar wire wound through the holes of a Fair-Rite 2843002402 binocular core, the details of which are shown in Fig. 9 (16, 17, 18). It helps to identify the three wires in the trifilar twist as being red, green and neutral. Now, both ends of the neutral wire are separated out to the right to form the primary winding. An opposite pair of red and green wires are joined together, and the remaining green and red wire ends then become the ends of the secondary winding. Referring again to Fig. 9, the upper left (or lower left) wire is connected to the transistor base and the lower right (or upper right) wire is connected to the transistor emitter.

Similarly, the Mini-Circuits T1-6T may be used for the second stage augmentation transformers T4 and T5, however a much better performing transformer is easily made with four turns of #32 bifilar wire wound along the outside of both holes of a Fair-Rite 2843002402 binocular core, the details of which are shown in Fig. 10 (16, 17, 18). It helps to identify the three wires in the bifilar twists as being red and green. At one end of the core the two green wires are joined together, while at the opposite end of the core the two red wires are joined together. Referring again to Fig. 10, the upper left (or lower left) wire is the input, which is connected to transformer T3. The lower right (or upper right) wire is connected to the transistor base, and the joined pair on the right is connected to the transistor emitter.

The manner in which transformer T4 is constructed presents an interesting design opportunity. As noted earlier, it has been found that in general the amplifier performance is best when the transformer turns ratio N is equal to

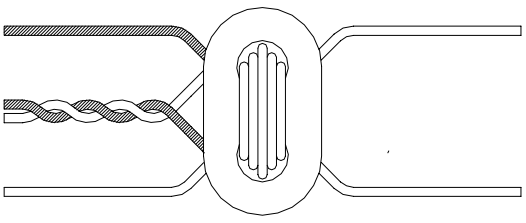

Fig. 9 - Transformer T1 Construction Details

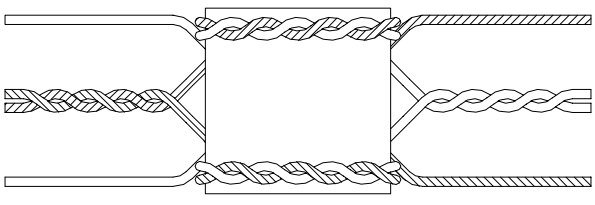

Fig. 10 - Transformer T4 Construction Details

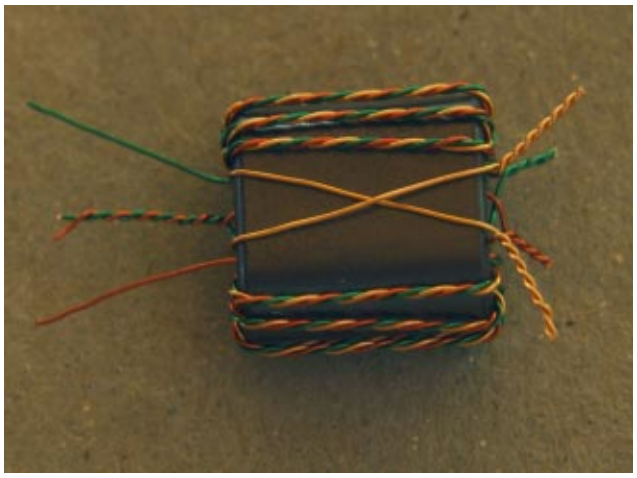

Fig. 11 - Transformer T6 Construction Details (bottom side shown)

1+M. In the construction described here, the upper bifilar pair of Fig. 10 is the M winding while the lower bifilar pair is the unity winding. Interconnecting the wires as described results in an M:1:N transformer. Therefore, the desgner can construc the transformer with the preferred ratios by simply adjusting the number of turns in the M winding.

Although the earlier discussion about transformers T3 and T6 may seem foreboding, their construction is rendered quite simple by way of careful attention to details. First, these transformers are identical in construction, which simplifies the logistics of the design. Six turns of #30 trifilar wire are wound along the outside of one hole of a Fair-Rite 2861000102 binocular core proceeding from the bottom surface to the top surface of the core. A second similar winding is then made along the outside of the second hole, again proceeding from the bottom surface to the top surface of the core.

As before, it helps to identify the three wires in the trifilar twist as being red, green and neutral. At one end of the core, the two red wires are joined together, and then the two green wires are joined together. The two neutral wires are the terminals of the secondary winding.

At the second end of the core, an opposite pair of red and green wires are joined together, forming the centre tap of the primary winding. The remaining opposite red and green wires are the end terminals of the primary winding. The neutral wires become the “cold” ends of the secondary windings of transformer T3 while for transformer T6 they are crossed over along the bottom surface to the opposite ends of the neutral wires on the first end of the core, effectively connecting the two windings in parallel as shown in Fig. 6. The photograph of Fig. 11 shows the construction of these transformers in detail, with T6 shown specifically so as to display the last step in its construction.

Note that 61 material is used for the cores of transformers T3 and T6. The 43 material used in the cores of the other four transformers has been found to be unsuitable for low-impedance circuitry due to excessive losses. For those wishing to make use of this design at low frequencies, all transformers should be made with cores of 73 material.

Input Roofing Filter Design

The input roofing filter consists of L1, C1, L2, C2, and C3. These last three components are unavoidable, capacitors C2 and C3 being blocking capacitors needed to isolate the emitters of transistors Q1 and Q2 from ground, as well as from each other so that the two devices do not need to be matched. Inductor L2 provides a ground connection for the loop antenna as well as ensuring that the amplifier input is balanced.

In many existing designs, these three components are simply made as large as practical to extend the low-frequency performance. In this design, the values are selected so as to provide an opportunity to filter out high power signals from LW and AM broadcast band stations that would cause interference by way of harmonics

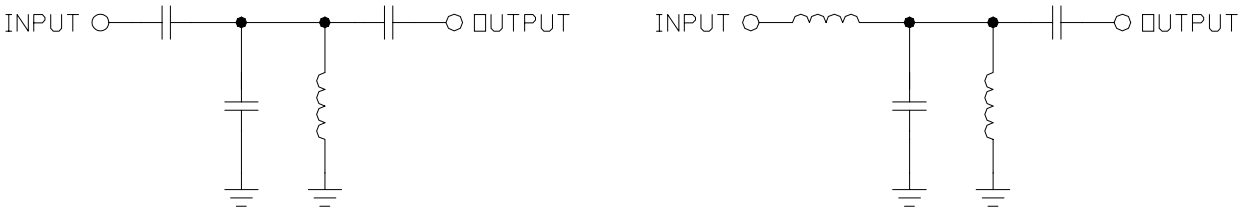

Fig. 12 - Coupled Resonator Bandpass Filter Evolution
from Unsymmetrical (left) to Symmetrical (right)

The remaining two components, L1 and C1, are optional and are included so as to provide the user with the opportunity to filter out high power signals from TV and FM broadcasters that might otherwise enter into the amplifier and cause interference by way of intermodulation products. The construction of L1 provides an additonal means for ensuring that the amplifier input is balanced. The values of the input roofing filter components will be discussed later.

When all five components are in use, the input roofing filter becomes a modification of the more familiar coupled resonator bandpass filter (19, 20, 21). In this class of filters, a series of parallel-resonant shunt circuits (resonators) are successively coupled by way of series capacitors. Such bandpass filters are convenient, however they are nor symmetrical. Each resonator represents a pole-zero pair, while each series capacitor is a zero. The consequence of this is that the filter is not symmetrical and suffers from poor stopband rejection above the passband.

By changing one series capacitor to a series inductor, the filter now has an equal number of poles and zeroes, and the response becomes symmetrical. Fig. 12 illustrates the evolution of this topology with a familiar unsymmetrical single resonator circuit shown

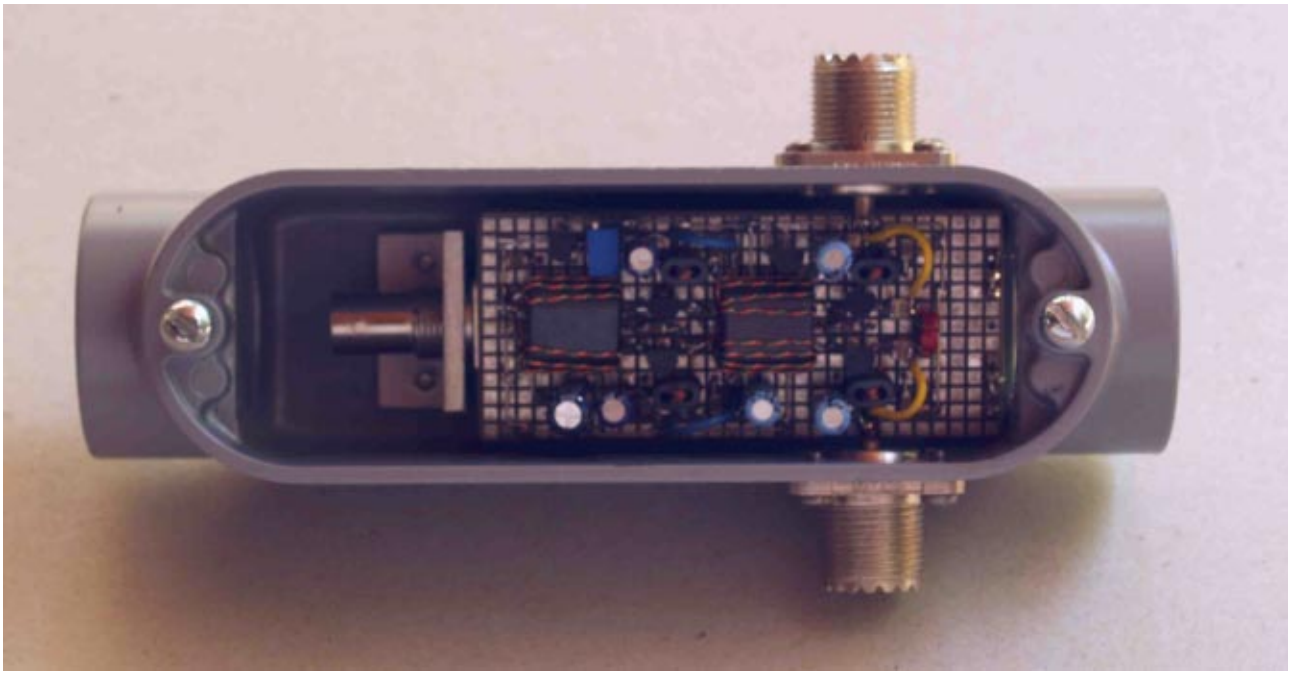

Fig. 13 - Earlier Ampliier Prototype Installed in 1” Metal Conduit Body

Table 2 - Roofing Filter LF Parts Values

C2, C3	L2	Frequency
0.10uF	82nH	887kHz
0.15uF	123nH	591kHz
0.22uF	180nH	403kHz
0.33uF	270nH	269kHz
0.47uF	385nH	189kHz
0.68uF	558nH	130kHz
1.00uF	820nH	87kHz

Table 3 - Roofing Filter HF Parts Values

C1	L1	Frequency
2700pF	3.9nH	34.7MHz
3000pF	4.3nH	31.2MHz
3300pF	4.7nH	28.4MHz
3900pF	5.6nH	28.4MHz
4700pF	6.7nH	24.0MHz
5600pF	8.0nH	16.7MHz
6800pF	9.7nH	13.8MHz

on the left and the modified symmetrical version shown on the right.

Prototype Construction and Testing

A prototype amplifier was constructed on a 1.3"x3.0" piece of Ivan Board (0.08" squares on 0.10" centres on 1/16" thick FR4 material with a solid ground plane). This size was dictated by the need to mount the amplifier inside a metal 1" electrical conduit body for use with shielded loop antenna elements. Fig. 13 is a photograph of the amplifier assembly as mounted in the conduit body with SO-239 connectors mounted on either side for attaching the loop antenna elements. A PCB-mounted right-angle BNC connector (Tyco 5227677-1) is mounted on the bottom side of the board, which is then mounted to an aluminum support bracket.

Note that in this photo components L1 and C1 are not installed and capacitors C4, C6, C11, C13, and C19 are 16V aluminum electrolytics. Also, this photo is that of an earlier prototype that used simple passive augmentation for the second stage where transformers T4 and T5 were the same as T2 and T3.

Inductor L2 is constructed with four turns of #32 bifilar wire on a T25-2 toroid, which gives an inductance of 100nH on each side. Capacitors C2 and C3 are American Technical Ceramics (ATC) 100B porcelain dielectric 0.1uF, which have a slightly better ESR than the X7R parts suggested in the parts list, but which are not readily available from popular distributors.

The values for resistors R1, R2, R3, and R4 were arrived at to provide a 20mA bias current for transistors Q1 and Q2, and a 30mA bias current for transistors Q3 and Q4. A 100-ohm 10-turn potentiometer was used for R6 for experimentation purposes.

Test were conducted to measure the amplifier input impedance , NF, and voltage gain at 10MHz, after which 2-tone tests were conducted using signals at 9.95MHz and 10.05MHz to measure the OIP2 and OIP3 performance. The results of these tests are listed in Table 4.

Table 4 - Amplifier Performance

Supply Voltage	12V
Supply current	120mA
Load resistance	50 ohms
Input Resistance	2.25 ohms
Voltage gain	+36dBv
OIP2	+80dBm
OIP3	+40dBm
NF	2.42dB

With the amplifier input resistance determined, a range of values for the input roofing filter was determined. The values available for C2 and C3 are somewhat limited, and Table 2

lists the inductance required for each half of L2 and the low-frequency cutoff that results. L2 is constructed as a bifilar twisted pair wound on a suitable powdered iron toroid that will result in at least four turns on a toroid of 1/4" outside diameter or more. The parts mentioned in the parts list of Fig. 5 for C2 and C3 have a suitable low ESR, but American Technical Ceramics (ATC) makes far better parts using a porcelain dielectric, though they are far more expensive and difficult to obtain. The low-frequency cutoff can be further improved by adding low ESR electrolytics in parallel with C2 and C3.

For the high-frequency cutoff function of the input roofing filter, the capacitor values are not as confining, but as shown in Table 3 the small value for each half of L1 is such that in some instances no toroid core will be needed and nothing more than a suitable length of a twisted pair of wire will be required. The parts list of Fig. 5 states that a mica capacitor be used for C1 as these have a very low ESR and are fairly easy to obtain. Better yet would be porcelain capacitors such as those made by ATC, as mentioned earlier for C2 and C3.

Closing Remarks

The amplifier described herein provides performance comparable to that of commercial units made by Wellbrook and Pixel, while costing considerably less. It also provided a suitable opportunity to demonstrate the input resistance, NF, and IMD performance that can be enjoyed with the use of passive augmentation.

References

1. Pan, S.-G., T. Becks, D. Heberling, P. Nevermann, H. Rösmann, and I. Wolff, “Design of Loop Antennas and Matching Networks for Low-Noise RF Receivers: Analytical Formula Approach,” *IEE Proceedings on Microwaves, Antennas, and Propagation*, Vol. 144, No. 4, August 1997, pp. 274-280.
2. King, R.W.P. and C.W. Harrison, *Antennas and Waves: A Modern Approach*, MIT Press, 1969.
3. Kraus, J.D., *Antennas, 2nd ed.*, McGraw-Hill, 1988.
4. Terman, F.E., *Electronic and Radio Engineering, 4th ed.*, McGraw-Hill, 1955.
5. Padhi, Trilochan, "Theory of Coil Antennas," *Journal of Research of the National Bureau of Standards*, Jul 1965, pp. 997-1001.
6. Storer, James E., "Impedance of Thin-Wire Loop Antennas," *AIEE Transactions*, Part 1, November 1956, pp. 606-619.
7. Awadalla, K.H. and A.A. Sharshar, "A Simple Method to Determine the Impedance of a Loop Antenna," *IEEE Transactions on Antennas and Propagation*, Vol. AP-32, No. 11, Nov 1984, pp. 1248-1251.
8. Flaig, T.L., "The Impedance and Efficiency of Multiturn Loop Antennas," Technical Report 2235-3, The Ohio State University Electroscience Laboratory, 3 April 1968.
9. Trask, C., "Active Loop Aerials for HF Reception, Part 1: Practical Loop Aerial Design," *QEX*, July/August 2003, pp. 35-42.
10. Streable, G.W. and L.W. pearson, “A numerical Study on Realizable Broad-Band and Equivalent Admittances for Dipole and Loop Antennas,” *IEEE Transactions on Antennas and Propagation*, Vol. 29, No. 5, September 1981, pp. 707-717.
11. Trask, C., "Common Base Amplifier Linearization Using Augmentation," *RF Design*, October 1999, pp. 30-34.
12. Trask, C., *Lossless Feedback Amplifiers with Linearity Augmentation*, US Patent 6,172,563, 9 January 2001.
13. Trask, C., *Common-Base Amplifiers with Linearity Augmentation*, US Patent 6,271,721, 7 August 2001.
14. Trask, C., "High Efficiency Broadband Linear Push-Pull Power Amplifiers Using Linearity Augmentation," *Proceedings of the 2002 International Symposium on Circuits and Systems* (ISCAS 2002), 28 May 2002, Phoenix, Arizona, Vol. 2, pp. 432-435.
15. Trask, C., "Active Loop Aerials for HF Reception, Part 2: High Dynamic Range Aerial Amplifier Design," *QEX*, Sep/Oct 2003, pp. 44-49.
16. Trask, C., "Wideband Transformers: An Intuitive Approach to Models, Characterization and Design," *Applied Microwave & Wireless*, Vol. 13, No. 11, November 2001, pp. 30-41.
17. Trask, C., “Designing Wide-band Transformers for HF and VHF Power Amplifiers,” *QEX*, May/April 2005, pp. 3-15.
18. Walker, John L.B., Daniel P. Meyer, Frederick H. Raab, and Chris Trask, *Classic Works in RF Engineering: Combiners, Couplers, Transformers, and Magnetic Amplifiers*, Artech House, 2006.
19. Huelsman, Lawrence P., *Active and Passive Analog Filter Design*, McGraw-Hill, 1993.
20. Zverev, Anatol I., *Handbook of Filter Synthesis*, Wiley, 1967.
21. Rosenbaum, G., “RF Capacitive-Coupled Filters,” *Applied Microwave & Wireless*, October 1998, pp. 74-83.